Minimum forebody drag in hypersonic continuum and rarefied flows

J. Pike
Bedfordshire, UK

ABSTRACT

Minimum drag shapes of given length and base area are investigated for hypersonic flow using both Newtonian impact theory and free molecular flow theory. The drag of Newton's minimum drag body, which has previously been evaluated by numerical means, is derived as an analytic expression. The analytical results are applicable to a range of local pressure laws allowing minimum drag shapes obtained using impact theory to be directly compared with low density flow equivalents using free molecular flow. The low density shapes are found to have larger blunt regions at the nose and significantly larger drag coefficients. For free molecular flow the drag varies with the surface reflection characteristics. As the fraction of diffuse reflection at the surface increases, the drag increases and the sensitivity of the drag to changes in the minimum drag shape is reduced.

NOMENCLATURE

a_o incident flow constant (Equation (17))
A cross-section area of body
C_d drag coefficient of incremental surface area with streamwise projected area as reference area (a function of x_r)
C_D drag coefficient with base area as reference area
k impact theory and specular reflection flow constant (Equation (11))
k_o,k_1,k_2 free molecular flow constants (Equation (22))
K_b shape constant (Equation (23))
F integrand of minimisation integral
F_x $\partial F/\partial x$
M_w molecular weight
r radius of axisymmetric body or the inscribed circle
$\Re$ universal gas constant
T temperature of gas or body surface
V free stream velocity
V_r specular reflection velocity
V_T molecular velocity at body surface temperature
x distance downstream from nose
x_r $dx/dr = \mathrm{Cot}\theta$
θ surface inclination angle to free stream direction
κ $2k_2/k_1$
ξ fraction of molecules reflecting specularly from a surface
τ $2r_b/x_b$

Subscripts

$(\,)_b$ base of body (at $x = b$)
$(\,)_o$ nose of body (at $x = 0$)

Paper No. 3023. Manuscript received 26 September 2005, revised version recieved 25 January 2006, accepted 25 April 2006.

https://doi.org/10.1017/S0001924000001287 Published online by Cambridge University Press

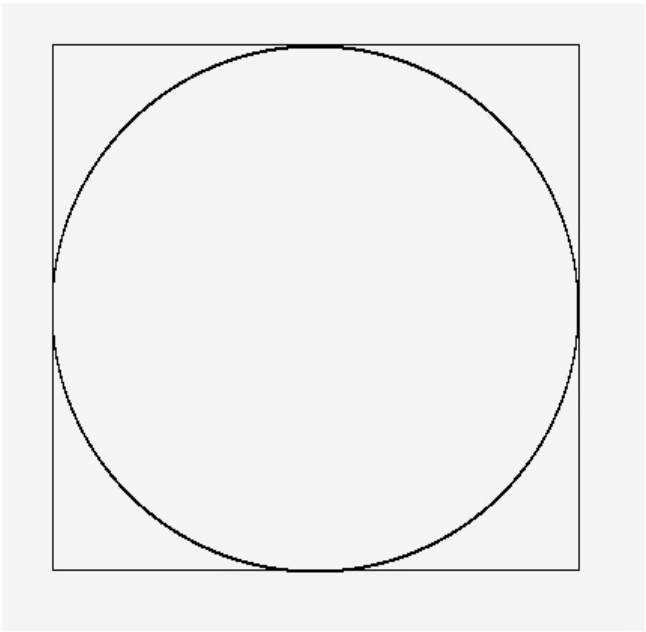


Figure 1. Square base shape with same minimum drag profile as the inscribed circle.

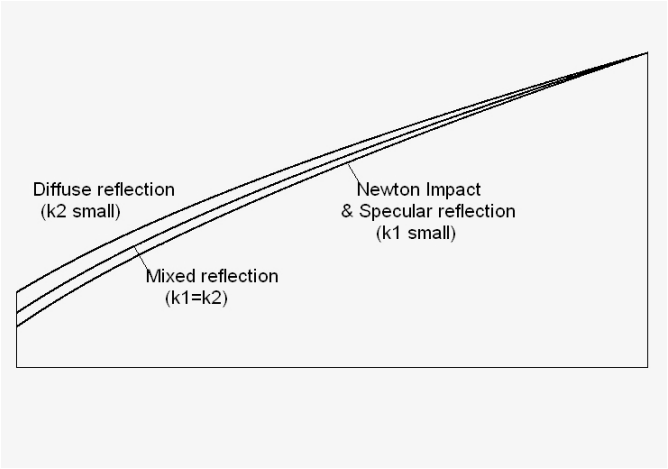


Figure 2. Minimum drag shapes for $\tau = 1$.

1.0 INTRODUCTION

The analysis of minimum drag shapes in hypersonic continuum[1-3] or free molecular flow[4-9], has identified low drag shapes and the potential for drag reduction at high speeds. Here for the constraints of given base shape and length, a range of results are obtained when the surface pressure is described by a local pressure law, that is when the surface pressure depends only on the local surface conditions and not on the history of the flow. Relevant examples are Newton's impact theory and free molecular flow theory, which are applicable to the flow at high Mach number and low density respectively. The use of impact theory at hypersonic speeds is well established for high density flows, although care is needed when using it for surface concavities and surfaces at small incidence to the flow. Any error at high incidence can be reduced by using modified Newtonian theory, where the maximum pressure coefficient (k) is based on the stagnation pressure instead of its infinite Mach number limit of two, although the error at small incidence remains. Low density hypersonic applications are less common, but such minimum drag shapes could, for example, extend the orbital life of a satellite in near earth orbit by reducing its drag, with particular application to micro-satellites or to maintaining the integrity of satellite constellations.

It is often required of bodies considered for minimum drag that the cross-sections are self similar along their length. The most important class of such bodies are axisymmetric bodies, but the minimum drag of bodies with other cross sections, such as regular polygons[6], are also of interest. The axisymmetric analysis is applicable to any self-similar cross-section where the cross-section shape is formed from tangents to an inscribed circle[6], as shown for example by the square cross-section shown in Fig. 1 (with typical profiles as shown in Fig. 2). The analysis also applies to tapered cylinders of given length and base where the inscribed radius at the nose (r_o) is specified rather than optimised, as it is for the minimum drag forebody. When the sections are not required to be self-similar along the body, a further reduction in the drag may be achievable by the use of spatular body shapes[3]. Although the drag of some spatular shapes may be obtained analytically, the drag of the minimum drag spatular body requires numerical evaluation.

A number of results already exists for axisymmetric and other minimum drag bodies using impact theory[1-3], and some results exist for free molecular flow theory[4-9]. However the minimum drag shapes from both impact theory and free molecular flow theory require numerical integration to evaluate the drag. Here by using the inverse of the surface slope as the parametric variable, a simple general analysis is obtained which is applicable to any integrable local pressure law, which allows a wider range of bodies to be treated analytically and gives expressions for the shape and minimum drag of these bodies.

1.1 Newton's minimum drag body

Included in the axisymmetric constraints is the well known problem of the minimum drag of an axisymmetric forebody of given slenderness ratio in hypersonic flow. The minimum drag shape for a body with a circular base and given length was originally obtained in the 1600s by Newton[1] using impact theory. The parametric equations of the minimum drag surface profile in terms of the surface slope dr/dx are well known[2,10].

i.e.
$$r = r_o \frac{\left(1+\left(\mathrm{d}r/\mathrm{d}x\right)^2\right)^2}{4\left(\mathrm{d}r/\mathrm{d}x\right)^3}$$

$$x = \frac{r_o}{4}\left(\frac{3}{4\left(\mathrm{d}r/\mathrm{d}x\right)^4}+\frac{1}{\left(\mathrm{d}r/\mathrm{d}x\right)^2}-\frac{7}{4}+\mathrm{Ln}\left(\mathrm{d}r/\mathrm{d}x\right)\right)$$

These same equations in terms of the inverse of the surface slope used here become;

$$r = r_o\left(1+x_r^2\right)^2/4x_r \qquad \ldots (1)$$

$$x = r_o\left(3x_r^4+4x_r^2-7-4\mathrm{Ln}\left(x_r\right)\right)/16 \qquad \ldots (2)$$

https://doi.org/10.1017/S0001924000001287 Published online by Cambridge University Press

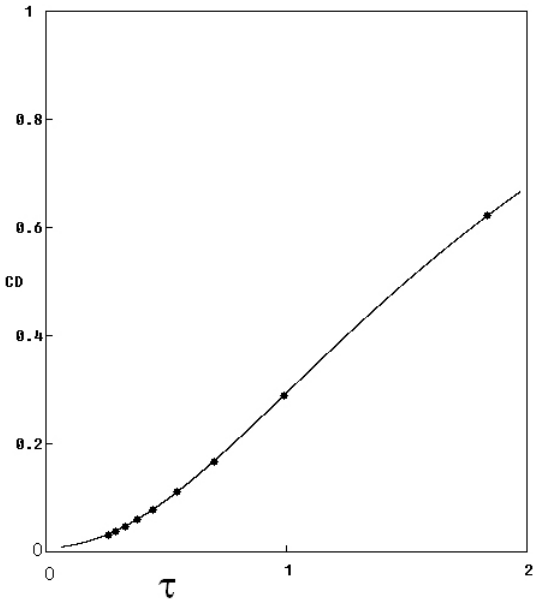


Figure 3. Drag coefficient of minimum drag axisymmetric forebodies using impact theory.

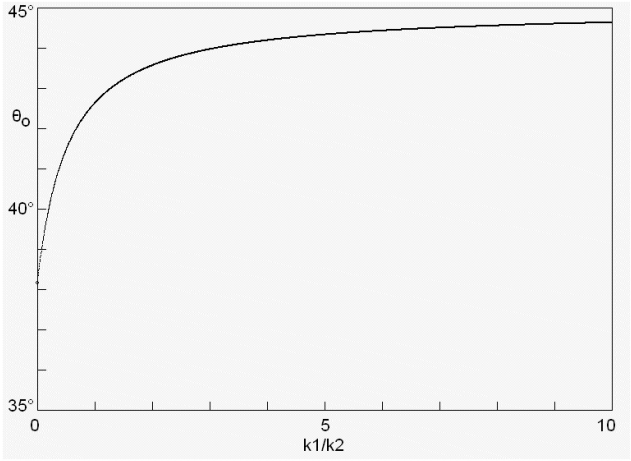


Figure 4. Initial surface slope versus the specular/diffuse fraction for free molecular flow.

where x_r is dx/dr for the surface. An axisymmetric shape corresponding to Equation (1) and (2) is shown in Fig. 2 for Newtonian impact theory. The variation of the cross-section area of the body is given from Equation (1) by;

$$A = A_o(1+x_r^2)^4/16x_r^2 \qquad \ldots (3)$$

where A_o is the blunt area at the nose of the body shown to the left in Fig. 2. Equation (3) gives the variation of the cross-sectional area of the minimum drag bodies such as that shown in Fig. 1.

The drag coefficient for a base radius r_b and a surface profile $r(x)$, is given by;

$$C_D = \frac{2\pi}{A_b}\int_0^{r_b} rC_d\,\mathrm{d}r = \frac{1}{A_o}\int_0^{A_b} C_d\,\mathrm{d}A \qquad \ldots (4)$$

where C_d is the drag coefficient of a small element with its streamwise projected area as reference area. Note that when $r<r_o$ the drag is that of the blunt region at the nose. When only normal forces act on the surface, such as for impact theory, the elemental drag increment is equal to the local pressure coefficient. Substitution for r from Equation (1) and C_d from impact theory into Equation (4) gives the drag of Newton's minimum drag body in integral form. This integral has been integrated numerically, to give, for example[3], the drag coeffients shown by the black circles in Fig. 3, but the drag has not previously been expressed analytically.

1.2 General analysis for minimum drag bodies with self-similar cross-sections

Consider bodies with cross sections formed from tangents to an inscribed circle (e.g. Fig. 1), in a flow where the surface pressures can be represented by a local pressure law. The streamwise co-ordinate downstream from the nose is given by x with the body base at x_b. The body profile is given by the radius of the inscribed circle r as some function of x, with radius r_o at the nose and r_b at the base. It could be assumed that the length x_b and base radius r_b are given, but for the present analysis it is only necessary to specify their ratio as $\tau = 2r_b/x_b$.

The minimisation of the drag uses the calculus of variations, where the application to body shapes is described in Refs 10 and 11. From the calculus of variations[2,10,11], the minimum drag profile satisfies Euler's equation;

$$\text{i.e.} \qquad F_x - \frac{\mathrm{d}}{\mathrm{d}r}F_{x_r} = 0 \qquad \ldots (5)$$

where F is the integrand of Equation (4), that is $rC_d(x_r)$, and the subscripts refer to the partial differential variable. Substituting for F and noting that it does not contain x explicitly, we have F_x is zero and hence;

$$rdC_d/dx_r = \mathrm{C} \qquad (6)$$

where C is a constant. The value of C can be obtained from Equation (6) by substituting the slope of the body at the base and also relates to conditions at the nose;

$$\text{i.e.} \qquad \mathrm{C} = r_b\left(\frac{\mathrm{d}C_d}{\mathrm{d}x_r}\right)_b = r_o\left(\frac{\mathrm{d}C_d}{\mathrm{d}x_r}\right)_o \qquad \ldots (7)$$

For the minimum drag body, the value of the inverse slope at the nose can be obtained by considering a small section of depth dx at the front of the body. Let the radius at a distance dx downstream be r_1 and the cross-section area be A_1 ,then the drag of the blunt nose of the body plus the drag of the section dx with slope $1/x_{ro}$ is given by;

$$D_1 = A_o\,C_d(0) + (A_1 - A_o)\,C_d(x_{ro})$$

Noting that;

$$1 - \frac{A_o}{A_1} = 1 - \frac{r_o^2}{r_1^2} = 1 - \frac{(r_1 - dr)^2}{r_1^2} = \frac{2dx}{r_1 x_{ro}} + O\left(dr^2\right)$$

and differenciating with respect to x_{ro} we obtain at the minimum;

$$C_d\left(x_{ro}\right) - x_{ro}\left(\frac{\mathrm{d}C_d}{\mathrm{d}x_r}\right)_o = C_d\left(0\right) \qquad \ldots (8)$$

https://doi.org/10.1017/S0001924000001287 Published online by Cambridge University Press

With x_{ro} from Equation (8), the radius of the flat region at the nose r_o can be obtained from Equation (7). Alternatively for a minimum drag tapered cylinder where the nose radius is fixed, the minimum drag profile is again given by Equation (6), with x_{ro} being determined from Equation (7). With $r(x_r)$ known from Equation (6), the variation of x with x_r is given from the definition of x (in terms of x_r) and integration by parts

$$\text{i.e.} \quad x = \int_{r_o}^{r} x_r dr = r x_r - r_o x_{ro} - \int_{x_{ro}}^{x_r} r dx_r \qquad \ldots (9)$$

On evaluation of the integral in Equation (9), Equations (6) and (9) give a parametric representation of the body profile for minimum drag, with x_r as the parameter. Equivalents of these equations have been solved in some cases previously[2,4,5] to give the shape but not the drag. The simplicity of Equations. (6) and (9) allows the range of shapes to extended and the drag to be calculated.

The drag coefficient for these bodies is obtained as an analytic expression from Equation (4) by integrating by parts and substituting from Equations (6) and (9).

$$\begin{aligned} r_b^2 C_D &= C_d(0) r_o^2 + 2\int_{r_o}^{r_b} r C_d \, dr \\ &= C_d(0) r_o^2 + [r^2 C_d]_{r_o}^{r_b} - \int r^2 (dC_d/dx_r) dx_r \\ &= r_o^2 (C_d(0) - C_d(x_{ro})) + r_b^2 C_d(x_{rb}) - C\int_{r_o}^{r_b} r dx_r \\ &= r_o^2 (C_d(0) - C_d(x_{ro})) + r_b^2 C_d(x_{rb}) - C(r_b x_{rb} - r_o x_{ro} - x_b) \end{aligned}$$

i.e.

giving the drag coefficient for a minimum drag tapered cylinder. For the minimum drag body, using Equation (8) for x_{ro} we obtain more simply;

$$C_{D\min} = C_d(x_{rb}) + (x_b/r_b - x_{rb})(dC_d/dx_r)_b \qquad \ldots (10)$$

giving the minimum drag coefficient as an analytic function of x_{rb}, the inverse of the surface slope at the base.

2.0 APPLICATIONS

2.1 Newtonian impact theory or specular reflection

For Newtonian Impact theory, the pressure coefficient is given by;

$$C_p = k\mathrm{Sin}^2\theta = k/(1+x_r^2) \qquad \ldots (11)$$

The same relationship with a different value of k holds in free molecular flow for the specular reflection of molecules from the surface for a body travelling at high speed, that is when the incident velocity of the molecules is large compared with the thermal velocity. For impact theory the value of k is normally taken to be two (or the stagnation pressure coefficient). For specular reflection where the reflected molecules have the same velocity as the incident molecules, the value of k is four. The value of the constant k in Equation (11) does not effect the minimum drag shape[9], which is described for both cases for Newton's minimum drag body by Equations (1 and 2), but the minimum drag coefficient is proportional to the value of k.

Note that from Equation (11) the variables θ and x_r are interchangeable, and although it is easier to do the analysis in terms of x_r it is simpler to express the derived results in term of the angle of inclination of the surface to the stream.

To find the drag coefficient from Equation (10), we have from differentiating Equation (11) with respect to x_r;

$$dC_d/dx_r = dC_P/dx_r = -2kx_r/(1+x_r^2)^2 = -2k\mathrm{Sin}^3\theta\,\mathrm{Cos}\theta \qquad \ldots (12)$$

giving from Equation (10);

$$C_{D\min} = k\mathrm{Sin}^2\theta_b (1 - (4/\tau)\mathrm{Sin}\theta_b \mathrm{Cos}\theta_b + 2\mathrm{Cos}^2\theta_b) \qquad \ldots (13)$$

The forebody ratio (τ) is given from Equations (1) and (2) in terms of θ_b by;

$$\tau = \frac{2r_b}{x_b} = \frac{8\mathrm{Tan}\theta_b}{3 - 2\mathrm{Sin}^2\theta_b - 4\mathrm{Sin}^4\theta_b (2 - \mathrm{LnTan}\theta_b)} \qquad \ldots (14)$$

Thus from Equations (13 and 14), the drag of Newton's minimum drag shape[1] is given directly as an analytic function of the surface inclination at the base.

i.e.

$$C_{D\min} = \frac{1}{2} k\mathrm{Sin}^2\theta_b (3 + \mathrm{Sin}^2\theta_b - 2\mathrm{Sin}^4\theta_b + 4\mathrm{Sin}^4\theta_b \,\mathrm{Cos}^2\theta_b (2 - Ln\mathrm{Tan}\theta_b)) \qquad \ldots (15)$$

The drag coefficient from Equations (15) and (14) is shown by the continuous line in Fig. 3 to agree with the numerically integrated results shown by the black circles.

Equations (15 and 14) also hold for specular reflection, when the reflected velocity is equal to the incident velocity and k has the value four. It can also be extended to include the case where the reflection velocity (V_r) differs from the incident velocity. In this case there is a tangential component of the transferred momentum such that the incremental drag coefficient is given by;

$$C_d = 2(1 - V_r/V) + 4(V_r/V)\,\mathrm{Sin}^2\theta$$

Thus from Equation (10) the minimum drag coefficient given in Equation (15) is still applicable with the addition of a constant $2(1-V_T/V)$ term and k equal to $4V_r/V$.

2.2 Diffuse reflection

For diffuse reflection from the surface, the molecules are reflected in a random direction away from the surface at a mean velocity V_T, where the magnitude of V_T depends on the surface temperature. For complete accommodation, when the temperature of the reflected molecules is equal to the surface temperature we have;

$$V_T = \sqrt{3\Re T / M_w} \qquad \ldots (16)$$

For random reflection the mean momentum transfer is normal to the surface and is given by the mass times $V_T/2$. Other reflection distributions have been suggested[12] giving slightly different values for the reflection momentum transfer, but as will be shown, the exact value of this parameter is not important at hypersonic Mach numbers. The pressure coefficient is then given by

$$C_P = a_o + (V_T/V)\mathrm{Sin}\theta \qquad \ldots (17)$$

where the constant a_o is due to the incident molecules, which have no effect on the shape of the minimum drag surface.

The usual and most important surface temperature assumption is that of a constant temperature. However before analysing this case it is worth noting that when the body surface temperature varies with body surface incidence as $\mathrm{Sin}^2\theta$, then from Equation (16), V_T varies as $\mathrm{Sin}\theta$ and via Equation (17) the minimum drag shape is conveniently the same as that for specular reflection and continuum hypersonic flow.

For constant surface temperature case, when V_T is constant we have from Equation (17);

$$dC_d/dx_r = dC_P/dx_r = -(V_T/V)x_r/(1+x_r^2)^{3/2} = -(V_T/V)\mathrm{Sin}^2\theta\,\mathrm{Cos}\theta \qquad \ldots (18)$$

whence from Equations (6) and (9), shape equations equivalent to

https://doi.org/10.1017/S0001924000001287 Published online by Cambridge University Press

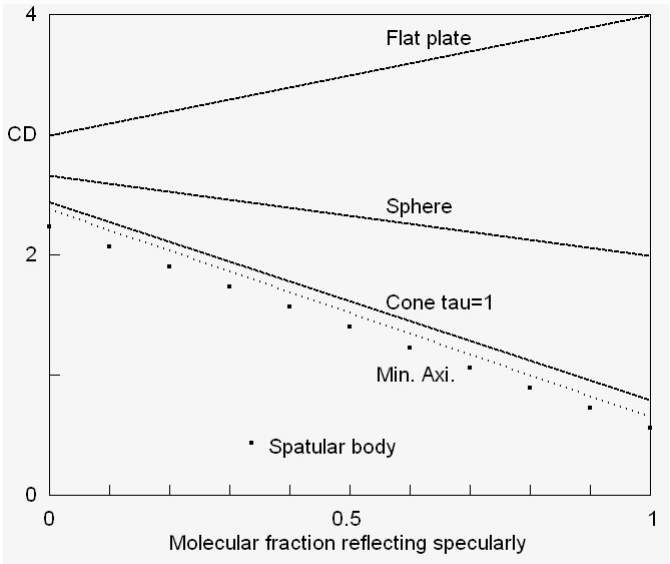


Figure 5. Drag coefficients of forebodies at equilibrium temperature.

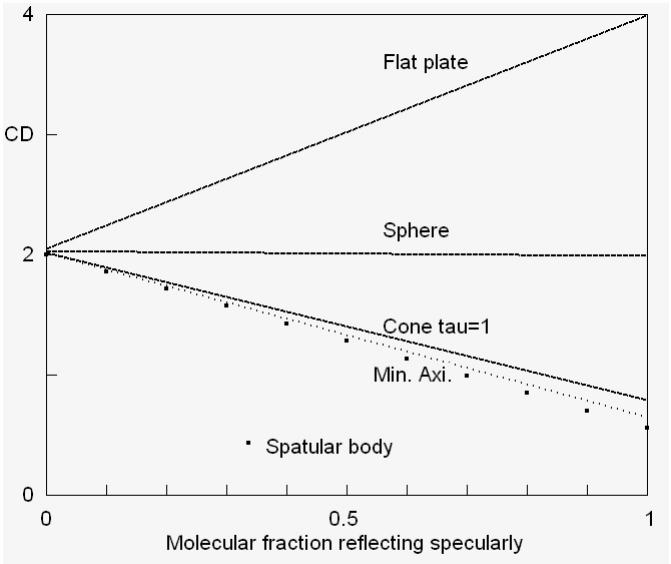


Figure 6. Drag coefficients of forebodies at lower temperatures.

those of Ref. 5 are given by;

$$r\mathrm{Sin}^2\theta\ \mathrm{Cos}\theta = r_b\mathrm{Sin}^2\theta_b\mathrm{Cos}\theta_b \qquad \ldots (19)$$

and;

$$x = r_b\mathrm{Sin}^2\theta_b Cos\theta_b\left[\frac{2}{3\mathrm{Sin}^3\theta}-\frac{1}{\mathrm{Sin}\theta}-\frac{1}{2}Ln\left(\frac{1-\mathrm{Sin}\theta}{1+\mathrm{Sin}\theta}\right)-1{\cdot}928\right] \qquad \ldots (20)$$

with the surface slope at the nose given by Sin $\theta_o = (\sqrt{5}-1)/2$. The profile for $\tau = 1$ is shown on Fig. 2. The drag coefficient is given analytically from Equation (10) as;

$$C_{D\min} = a_o + (V_T/V)\mathrm{Sin}\theta_b\,(1-(2/\tau)\mathrm{Sin}\theta_b\mathrm{Cos}\theta_b + \mathrm{Cos}^2\theta_b) \qquad \ldots (21)$$

where the momentum of the incident molecules requires $a_0 = 2$.

2.3 Free molecular flow

The specular and diffuse reflections considered previously gave different minimum drag body shapes and drags. In free molecular flow the surface reflections can be modelled as a merging of the above cases, commonly as a linear combination. That is we assume a fraction ξ of the molecules reflect specularly and a fraction $1 - \xi$ diffusely. Then for an incremental drag coefficient of the form

$$C_d = k_0 + k_1\mathrm{Sin}\theta + k_2\mathrm{Sin}^2\theta \qquad \ldots (22)$$

the linear combination constant values are given by $k_0 = 2(1 - \xi V_r/V)$, $k_1 = (1-\xi)V_T/V$ and $k_2 = 4\xi V_r/V$. Note that the minimum drag shape depends only on the ratio of k_1 to k_2 and is independent of k_0. That is;

$$r\mathrm{Sin}^2\theta\ \mathrm{Cos}\theta(k_1 + 2k_2\mathrm{Sin}\theta) = r_b\mathrm{Sin}^2\theta_b\mathrm{Cos}\theta_b(k_1 + 2k_2\mathrm{Sin}\theta_b) = K_b \qquad \ldots (23)$$

$$x = K_b(f(\mathrm{Sin}\theta) - f(\mathrm{Sin}\theta_o)) \qquad \ldots (24)$$

where with $\kappa = 2k_2/k_1$, the function f is given by;

$$f(s) = \frac{1}{s^3(1+\kappa s)} - \frac{1}{3s^3} + \frac{\kappa}{2s^2} - \frac{1+\kappa^2}{s} + \kappa(1+\kappa^2)\mathrm{Ln}\left(1+\frac{1}{\kappa s}\right) - \frac{1}{2(1+\kappa)}\mathrm{Ln}\frac{\kappa(1-s)}{1+\kappa s}$$

$$+\frac{1}{2(1-\kappa)}Ln\frac{\kappa(1+s)}{1+\kappa s} \qquad \ldots (25)$$

The angle of the surface at the nose θ_o is from Equation (8) given by;

$$2\kappa\mathrm{Sin}^3\theta_o + 2(1+\kappa)\mathrm{Sin}^2\theta_o + (2-\kappa)\mathrm{Sin}\theta_o = 2+\kappa \qquad \ldots (26)$$

The variation of θ_o from diffuse to specular reflection is shown in Fig. 4 from Equation (26). As k_2/k_1 becomes large, θ_o tends to 45°. The drag coefficient of the minimum drag shape is from Equation (10)*i*;

$$C_{D\min} = 2(1-\xi V_r/V) + (1-\xi)V_T/V\,\mathrm{Sin}\theta_b\,(1-2/\tau\mathrm{Sin}\theta_b\mathrm{Cos}\theta_b + \mathrm{Cos}^2\theta_b)$$

$$+4\xi V_r/V\mathrm{Sin}^2\vartheta_b(1-4/\tau\mathrm{Sin}\theta_b\mathrm{Cos}\theta_b + 2\mathrm{Cos}^2\theta_b) \qquad \ldots (27)$$

The minimum drag depends on the surface temperature via the V_T term. If we assume equilibrium conditions at the surface, there is no heat transfer from the flow to the surface and the mean velocity of the diffusely reflected molecules is the same as the incident molecules. For $V_r = V$ the drag coefficient of a variety of shapes varying from a flat plate to the minimum drag shape are shown in Fig. 5. The non-optimum shapes are shown in the figure to illustrate the potential for drag reduction under various conditions. At the right hand axis the reflection conditions are fully specular and they vary to become fully diffuse at the left hand axis. The specular drag coefficients on the right hand axis are twice the drag coefficients predicted by impact theory for continuum flow. That is with specular reflection the flat plate normal to the flow has a drag coefficient close to four, the sphere drag coefficient is half of this value at two and the cone with $\tau = 1$ has a value of 0·8. Equation (27) with $\tau = 1$ gives a value of 0·66 for the optimum

https://doi.org/10.1017/S0001924000001287 Published online by Cambridge University Press

axisymmetric (or polygonal cross-section) shape and numerical optimisation gives[3] the minimum drag coefficient of a body of given length and circular base section (whose shape is constrained to remain convex) as 0·56. This spatular body shape also gives the lowest drag when a fraction of the molecules are reflected diffusely, as is shown by the individual dots with the lowest drag on Figs (5) and (6).

As the fraction of diffusely reflected molecules increases towards the left hand axis, the differences between the drag coefficients of the various shapes decreases. More importantly, there is a significant increase in the drag of the optimum shapes, until for all diffuse reflection the minimum drag is over twice the drag for specular reflection. Thus not only are the advantages of shaping the surface reduced for rough surfaces but also the minimum drag gets significantly larger as the surface gets rougher.

This increase in the drag with surface roughness can be important for satellites where the surface smoothness is degraded by dust impact through the life of the satellite. However for satellites the equilibrium surface temperature assumption used above (and in Refs. 7 and 8) may be unrealistic because it implies high surface temperatures. At very low density the surface temperature might more typically be related to the static temperature of the gas. However the particular value used is not critical because the drag results are insensitive to the value of this much lower temperature. With the static temperature assumption we have from Equation (16)

$$\frac{V_T}{V} = \frac{1}{M}\sqrt{\frac{3}{\gamma}} \qquad \ldots (28)$$

Taking Mach 25 as typical of the Mach number in low earth orbit and $\gamma = 1{\cdot}4$, the value of V_T/V becomes 1/17. Using this value for the surface temperature gives the drag coefficients shown in Fig. 6. The drag is the same for the specular case on the right hand axis, but for cases where part of the deflection is diffuse reflection the drag is less than that shown in Fig. 5, with the differences being most marked near the diffuse reflection axis. Very noticeable also is that near the diffuse axis the drag is nearly independent of the shape of the body. This result is true for any low temperature (i.e. temperatures measured in hundreds rather than thousands of degrees). Comparison of Figs. 5 and 6 shows that the minimum achievable drag increases with both the temperature of the surface and the fraction of diffuse reflection.

CONCLUSIONS

Analytic expressions for the minimum drag of axisymmetric bodies of given slenderness ratio are derived for local aerodynamic theories. The expressions are evaluated for

- Impact theory to give an analytic expression for the drag of Newton's classic minimum drag shape.
- Hypersonic free molecular flow theory to give the shape and drag for variable molecular reflection conditions.

The axisymmetric minimum drag is compared with the drag of non axisymmetric minimum drag shapes. It is shown that:

- the minimum drag coefficient is the same for bodies with cross-sections which are regular polygons
- relaxing the similar cross-section constraint results in spatular shaped bodies with smaller drag.

APPENDIX

Error in the drag estimate from neglecting the thermal motion in free molecular flow

The error introduced by neglecting the thermal motion of the molecules depends on whether the thermal velocity (c) is greater or less than the component of the free stream velocity normal to the surface (V_n). At satellite velocities in the upper atmosphere (M~25), the mean thermal velocity and the normal approach velocity will be equal for a surface inclined to the freestream of between 2° and 3°. As the momentum transfer in the streamwise direction also becomes small when the surface inclination is small we are interested almost exclusively in the errors when $c < V_n = V\mathrm{Sin}\theta$.

In this case, where the thermal velocity towards the surface is less than the normal flow velocity, the momentum normal to the surface of the incident molecules is given by $\rho(V_n^2 + c^2/3)$. Here c^2 is the mean square thermal velocity of the molecules and $c^2/3$ is the static pressure[14]. In this case the momentum transfer to the surface in the streamwise direction is increased by a factor $1 + c^2/3V^2$ by including the thermal velocity. For the reflecting molecules, the diffusely reflecting molecules reflect from the surface at the surface temperature, and hence their momentum contribution is only affected if the inclusion of the random velocity were to change the surface temperature. Specularly reflecting molecules have the momentum transfer increased by the same ratio as the incident molecules. Thus for surfaces which have significant inclination so that $c < V_n$, the error is $O(c^2/V^2)$ and may safely be neglected.

When $c > V\mathrm{Sin}\theta$ the error term is $O(c)$ and the thermal velocity can have a larger effect on the accuracy. Thus analysis which results in shapes with large surface area parallel to the flow might need to consider this error. However, none of the shapes discussed here would be affected unless τ i s very small.

REFERENCES

1. NEWTON, I. *Mathematical Principles of Natural Philosophy*, A. MOTTE'S translation revised by F. CALJORI, University of California Press, 1934, Berkeley, California, USA.
2. EGGERS, A.J. JN, RESNIKOFF M.M. and DENNIS D.H. Bodies of revolution having minimum drag at high supersonic airspeeds. NACA-TR-1306, 1 January 1957.
3. PIKE, J. Minimum drag bodies of given length and base using Newtonian theory, 1977, *AIAA J*, **15**, (6).
4. CARTER, W.J. Optimum nose shapes for missiles in the superaerodynamic region, *J Aeronautical Sciences*, July 1957, **7**, pp 527-532.
5. TAN, H.S. On optimum nose curves for superaerodynamic missiles. *J Aeronautical Sciences*, 1958, **25**, (4), pp 263-264.
6. PIKE, J. Forces on convex bodies in free molecular flow. *AIAA J*, November 1975, **13**, (11), pp 1454-1459.
7. BOWMAN, D.S. and LEWIS, M.J. Minimum drag power-law shapes for rarefied flow. *AIAA J*, **40**, (5), p 1013.
8. BOWMAN, D.S. and LEWIS, M.J. Optimization of low-perigee spacecraft aerodynamics. *J Spacecraft and Rockets*, **40**, (1), January-February 2003, pp 56-63.
9. DENNIS, D.H. On optimum nose shapes for missiles in the superaerodynamic region, *J Aeronaut Sciences*, Readers Forum, **25**, (3), p 216, March 1958.
10 RASMUSSEN, M. *Hypersonic flow*. John Wiley and Sons, New York, USA, 1994, p 297.
11. HAYES, W.F. and PROBSTEIN, R.F. *Hypersonic Flow Theory*, 2nd ed, Academic Press, 1966, Chapter III, pp 152.
12. GOODMAN, F.O. and WACHMAN, H.Y. *Dynamics of Gas-Surface Scattering*, Academic Press, New York, USA, 1976, pp 23,24.
13. ANDERSON, J.D. Jr *Hypersonic and High Temperature Gas Dynamics*, McGraw-Hill, New York, USA, 1989, pp 472.

https://doi.org/10.1017/S0001924000001287 Published online by Cambridge University Press